Cellular and Molecular Life Sciences

REVIEW

Optical probes and techniques for O_2 measurement in live cells and tissue

Ruslan I. Dmitriev · Dmitri B. Papkovsky

Abstract In recent years, significant progress has been achieved in the sensing and imaging of molecular oxygen (O_2) in biological samples containing live cells and tissue. We review recent developments in the measurement of O_2 in such samples by optical means, particularly using the phosphorescence quenching technique. The main types of soluble O_2 sensors are assessed, including small molecule, supramolecular and particle-based structures used as extracellular or intracellular probes in conjunction with different detection modalities and measurement formats. For the different O_2 sensing systems, particular attention is paid to their merits and limitations, analytical performance, general convenience and applicability in specific biological applications. The latter include measurement of O_2 consumption rate, sample oxygenation, sensing of intracellular O_2, metabolic assessment of cells, and O_2 imaging of tissue, vasculature and individual cells. Altogether, this gives the potential user a comprehensive guide for the proper selection of the appropriate optical probe(s) and detection platform to suit their particular biological applications and measurement requirements.

Abbreviations
CPP   Cell-penetrating peptides
EC   Extracellular
ecO_2 Extracellular O_2
FLIM Fluorescence/phosphorescence lifetime imaging microscopy
IC   Intracellular
icO_2 Intracellular O_2
NP   Nanoparticle(s)
OCR   Oxygen consumption rate
PEG   Poly(ethyleneglycol)
RLD   Rapid lifetime determination
TR-F Time-resolved fluorescence/phosphorescence

R. I. Dmitriev · D. B. Papkovsky (✉)
Biochemistry Department, University College Cork,
Cavanagh Pharmacy Building, Cork, Ireland
e-mail: d.papkovsky@ucc.ie

Introduction

It is hard to overestimate the significance of the measurement of molecular oxygen (O_2), particularly in biological samples containing respiring cells and tissues. Detailed understanding of the biological roles of O_2 is of major fundamental and practical importance [1, 2]. Being the key metabolite and the source of energy for mammalian cells, O_2 is used to produce ATP through the electron transport chain and oxidative phosphorylation process. It is also a substrate of numerous enzymatic reactions within the cell which are vital for its normal function, and can serve as a signal for genetic adaptation to hypoxia, for example through hypoxia-inducible factor (HIF) pathway [3, 4]. O_2 is a small, gaseous, non-polar analyte which has moderate solubility in aqueous solutions ($pO_2 = 160$ mmHg, or ~ 200 μM at 37°C). It is supplied to cells and tissues by passive diffusion and, in higher multicellular organisms, by convectional transport via vasculature, red blood cells and haemoglobin [3].

On the measurement side, the main parameters that require monitoring are (1) in situ oxygenation, (2) O_2 consumption rate (OCR), and (3) localised O_2 gradients within respiring samples, as well as the dynamics of these

parameters as a result of changes in cellular function. Under normal homeostatic conditions in vivo, these parameters are maintained within the defined physiological limits, with significant fluctuations seen in exercised muscles, brain tissue, and excitable cells [3]. OCR reflects the respiratory activity of the sample and, together with the other markers, such as ATP content, mitochondrial membrane potential, ion and metabolite concentrations and fluxes, the bioenergetic status of the cell. Deviations of the OCR from the norm are indicative of perturbed metabolism, mitochondrial dysfunction or disease state [5]. Similarly, changes in cell or tissue oxygenation are associated with many common pathological conditions including ischemia/stroke, cancer, neurological and metabolic disorders. Short-term and sustained hypoxia is known to induce rearrangement of cell metabolism, and ultimately lead to cell death or protection and adaptive responses (e.g. via Warburg effect, hypoxia-induced expression of genes and proteins such as HIF-1α, PGC-1α [4, 6, 7]). All this highlights the importance of O_2 measurement in biological samples containing respiring cells and tissue, and the need for corresponding tools and measurement methodologies to perform this in many different ways.

The area of O_2 measurement has been under active development over many years. Initially, it was boosted by the introduction of Clark-type oxygen electrodes [8], photometric (myoglobin) [9, 10] and EPR systems [11], which have been very useful in basic bioenergetic, metabolic, cell biology and toxicological studies with rather simple, macroscopic models. These techniques have been used with isolated mitochondria, suspension cells, and in point measurements in vivo [8]. More recently, they have been extended by microelectrodes [12–14], systems for adherent cells [15, 16], EPR probes [17, 18], ^{19}F MRI [19, 20], pimonidazole staining [21], and fibre-optic sensing [22], and enhanced by the technological advancements in analytical instrumentation [23].

Biological O_2 sensing techniques based on phosphorescence quenching and soluble probes, pioneered by David Wilson et al. [24], have opened new opportunities in the area. In the last decade, these systems have been revolutionised with a number of advanced sensor chemistries, measurement methodologies and instrumentation, thus enabling new analytical tasks and applications. In addition, several new optical sensing methods have been introduced, including the measurement of O_2-dependent fluorescence of GFP constructs [25] and imaging of delayed fluorescence [26]. While becoming more available and affordable for ordinary biomedical users, the existing platforms for optical sensing and imaging of O_2 in biological samples possess a number of special features and technical challenges, which require careful consideration in their selection and use.

Here, we review the available range of optical O_2 probes and detection platforms designed for biological samples and applications, with particular focus on quenched-luminescence O_2 sensing and imaging techniques. The main types of O_2 sensing materials, detection modalities, and biological applications are analysed and cross-compared. This is aimed at giving potential users a comprehensive guide for how to select an appropriate measurement platform for their particular biological object, instrumentation available and analytical task pursued.

Principles of O_2 sensing by photoluminescence quenching

Dynamic quenching of luminescence by O_2 involves a collisional interaction of O_2 molecules with the luminophore in its lowest excited state, resulting in radiationless deactivation and return to the ground state. As a result, luminescence intensity (I) and lifetime (τ) are both reduced in the presence of O_2 according to the Stern–Volmer equation [27]:

$$I_0/I = \tau_0/\tau = 1 + K_{s-v} \times [O_2] = 1 + k_q \times \tau_0 \times [O_2], \quad (1)$$

where I_0 and τ_0 are unquenched intensity and lifetime at zero O_2, respectively, K_{s-v} is the Stern–Volmer quenching constant, and k_q the bimolecular quenching rate constant, which depends on the immediate environment of the reporter dye, temperature and sterical factors. Each O_2-sensitive luminescent material has a characteristic relationship between $[O_2]$ and τ (or I). Luminescence lifetime is an average time which the luminophore stays in the excited state before emitting a photon. It is equal to the reciprocal of the excited state deactivation rate constant. This characteristic is independent of the concentration, and therefore lifetime measurements are the preferred luminescent parameter for sensing, from which O_2 can be quantified as follows:

$$[O_2] = (\tau_0 - \tau)/(\tau \times K_{s-v}) \quad (2)$$

For an ideal situation (solution-based systems), the Stern–Volmer plot of $[O_2]$ versus τ^{-1} is linear, and this allows for simple two-point calibration. However, many existing O_2-sensitive materials show heterogeneity and a non-linear Stern–Volmer relationship [28].

Since the analytical relationship between the primary luminescent parameter (I or τ) and O_2 concentration is hyperbolic, maximal sensitivity to O_2 (dI/dO_2 or $d\tau/dO_2$) is always at zero O_2. To achieve good measurement resolution in a given O_2 range (for in vitro studies, this range is usually 0–250 μM, while in vivo −0 to 50 μM), probe luminescence should be moderately quenched (approximately 2- to 5-fold) [29]. This requirement sets the following optimal values for the K_{s-v}: approximately

10 mM^{-1} at 200 μM O$_2$ or 100 mM^{-1} at 20 μM O$_2$. Probes with much higher or much lower K_{s-v} values will have a reduced performance due to small signal changes by O$_2$.

A calibration experiment involves measurement of the probe signal (τ or I) at several known O$_2$ concentrations, usually at 37°C for animal cell samples or 30°C for microbial, environmental samples, and fitting the data points to determine the [O$_2$] = $f(\tau)$. Under equilibrium conditions, the concentration of O$_2$ in solution and solid films is related to the partial pressure in the gas phase according to Henry's law.

A noteworthy factor is that a major by-product of the quenching process is singlet oxygen—a reactive, but rather short-lived form of O$_2$ which mostly returns back to the ground (triplet) state O$_2$. However, singlet oxygen can also react with nearby molecules, including the dye and sample components (lipids, proteins, nucleic acids), and thus affect the sensor, sample and measurement [30].

Oxygen-sensitive materials

The luminescent O$_2$ sensing materials described so far can be classified according to a number of criteria.

The reporter dye

Phosphorescent Pt(II)- and Pd(II)-porphyrins are among the most popular in O$_2$ sensing [24, 29, 31, 32]. These dyes exhibit phosphorescence lifetimes in the range of 40–100 μs for Pt-porphyrins and 400–1,000 μs for Pd-porphyrins, which provide them moderate to high quenchability by O$_2$. They have intense absorption bands in the UV (370–410 nm) and visible (500–550 nm) regions, and bright, well-resolved emission (630–700 nm) which is retained at ambient temperatures and in aqueous solutions

[32]. This makes Pt-porphyrins well suited for the ambient O$_2$ range (0–200 μM), and Pd-porphyrins—for the low O$_2$ range <50 μM. Quenchability by O$_2$ can be tuned by changing the micro-environment of the dye, for example by conjugating it to a macromolecular carrier [33], surrounding it with a dendrimeric shell [31] or embedding it in a suitable polymer. A number of related dye structures have been developed, including the phosphorescent Pt and Pd complexes of benzoporphyrins and porphyrin-ketones [31, 34, 35], which show longwave-shifted excitation bands (590–650 nm), emission at 730–900 nm (better suited for tissue imaging), and greater brightness [34, 36]. The highly photostable PtPFPP dye is actively used in a number of O$_2$ sensing probes [37]. Unlike the highly phototoxic PDT drugs and photosensitizers of porphyrin origin (e.g. photofrin, chlorins, precursor 5-aminoluvulenic acid), the porphyrin dyes used in existing extracellular and intracellular oxygen probes rarely show significant phototoxic action on mammalian cells and tissue under standard (optimised) measurement conditions [38–41]. This, however, needs to be carefully monitored in each case.

Besides the porphyrins, phosphorescent Ru (II) complexes have been used in biological O$_2$ sensing and imaging systems [42, 43]. These cationic dyes have good photostability and moderate brightness (lower than the porphyrins), while their lifetimes are significantly shorter (1–5 μs).The latter results in a lower sensitivity to O$_2$, thus requiring special polymeric matrices. On the other hand, shorter lifetimes provide faster signal acquisition rates in TR-F detection and fluorescence imaging (see below). Cyclometallated complexes of Ir(III) also show convenient spectral characteristics, high brightness and medium range lifetimes, compared to Pt-porphyrin and Ru(II) dyes [44, 45]. However, modest photostability limits their use in O$_2$ sensing and imaging systems. The characteristics of some common indicator dyes used in biological O$_2$ sensing systems are given in Table 1.

Table 1 Phosphorescent characteristics of some common dyes used in O$_2$ sensing

Indicator dye	Excitation optimum (nm)	Emission optimum (nm)	Lifetime τ_0 (μs)	Quantum yield/ solvent	Refs.
PdTPCPP	415, 524	690	~800	~0.1/water	[31]
PdTCPTBP	442, 632	790	240	0.12/water	[31]
PtCP	380, 535	650	~60	0.28/water	[46]
PtTBP	416, 609	745	50	0.50/DMF	[47]
PtCPK	400, 596	767	24	0.01/water	[36]
Ir(III)(C$_x$)$_2$(acac)	472, 444	563	11.3	0.54/CHCl$_3$	[45]
[Ru(bpy)$_2$(picH$_2$)]$^{2+}$	460	607	0.7–0.9	0.07/water	[42, 48]

PdTPCPP Pd(II)-meso-tetra-(4-carboxyphenyl)porphyrin, *PdTCPTBP* Pd(II)-meso-tetra-(4-carboxyphenyl)tetrabenzoporphyrindendrimer, *PtCP* Pt(II)-coproporphyrin, *PtTBP* Pt(II)-meso-tetrabenzoporphyrin, butyl octaester, *PtCPK* Pt(II)-coproporphyrin-ketone, *Ir(III)(Cx)$_2$(acac)* cyclometalatedIr(III) μ-chloro-bridged dimer coumarin complex, *[Ru(bpy)$_2$(picH$_2$)]$^{2+}$* [Ru(bpy)$_2$(2-(4-carboxyphenyl)imidazo-[4,5-f][1,10]phenanthroline)H$_2$)]$^{2+}$

Probe structure

The main forms of sensor materials are the *solid-state coatings* and *probes* (water-soluble reagents).These two are bridged by the *particulate sensors* which in the context of this review we also regard as probes. Solid-state sensors are usually used in O_2 microsensors [12], sensor coatings [49] and integrated systems [50]. They provide reliable and accurate measurement of extracellular O_2 (see below), but have limited flexibility. These systems have been reviewed extensively [29, 51, 52] and are outside the scope of this review.

Within the group of O_2 probes, several categories can be defined. The *small molecule probes*, represented by PdTPCPP [53, 54], Ru(II) dyes [42, 48] and PtCP derivatives [55], comprise hydrophilic dye structures having good solubility in aqueous media provided by the carboxylic and sulfonate groups. However, such probes have a tendency to non-specifically bind to proteins, cells and surfaces (due to hydrophobic regions in their structure), migrate to different locations within the sample and/or show cross-sensitivity to sample composition (pH, ionic strength, protein content).

These issues were partly addressed by developing the *supramolecular probes* in which several distinct functionalities are covalently linked together in one chemical entity. For example, conjugations of an O_2 sensitive dye to a hydrophilic macromolecular carrier such as protein or PEG [32, 54, 56] help make the probe cell-impermeable and keep it in solution, tune the sensitivity to O_2 and stabilise the calibration. MitoXpress^{TM} probe [33] from this category is now actively used in respirometric screening assays with isolated mitochondria, adherent and suspension mammalian and microbial cells [57], small organisms, and with compound libraries and environmental samples [58, 59].

The cell-impermeable dendritic probes have been developed by the Vinogradov group for imaging of tissue and vasculature [31]. In such structures, the central moiety of meso-substituted Pd/Pt-porphyrin or benzoporphyrin is modified via four peripheral carboxylic groups with dendritic polyglutamic chains that shield the phosphor from interferences (quenchers, pH, ionic strength) and reduce its quenchability by O_2. Incorporation of an additional hydrophilic shell by PEGylation of these dendrimeric structures improves their water solubility. Thus far, several such probes have been produced which span the excitation wavelengths from 400 to 700 nm and emission wavelengths from the red to near-infrared, and have different sensitivities to O_2 [35].

Another group of supramolecular probes are conjugates of the phosphorescent dyes with cell-penetrating peptides (CPP) for sensing intracellular O_2 [42, 60–62]. In this case, the luminescent moiety [a Ru(II) dye or Pt-coproporphyrin (PtCP)] is linked to a targeted delivery vector, such as

polyarginine or proline-rich peptides which escort the whole structure into the cell by passive means and retain it inside [63]. The conjugation improves the functional properties of the probe with the possibility of sensing intracellular O_2 gradients, and allows simple analysis of cell populations on a commercial fluorescent reader. Modest photostability of the existing conjugates (mostly PtCP based) makes them difficult to use in O_2 imaging. In the future, this limitation can be addressed by developing new conjugates based on more photostable and/or brighter dyes (e.g. PtCPK and PtTCPTBP derivatives [36, 47]), and nanoparticle formulations with highly photostable non-functionalised dyes such as PtTFPP and targeted delivery features (see below).

Micro- and nanoparticle (NP) based probes are now under active development [64–67]. These probes with covalent or non-covalent incorporation of the dye usually have larger size (polymeric) and variable composition (distribution). Fabrication methods include impregnation of commercial polymeric beads (e.g. polystyrene), inclusion of indicator dyes during emulsion polymerisation [68] and formation of core–shell nanostructures by a precipitation method [67]. The NP technology provides greater flexibility with indicator dyes: hydrophobic structures lacking functional groups (i.e. not suitable for the other probe types) and pairs of dyes (ratiometric or FRET based O_2 sensing) can be used in such systems [69, 70]. A number of new and well-known biocompatible polymers and co-polymers have been tested, such as polystyrene, polyfluorene and hydrogels. Furthermore, surface modification, for example, altering the surface charge of the NPs or adding a special peptide coat, allows optimisation of their specificity, and penetration into or exclusion from the cell [64, 67, 69, 71, 72]. The advantages of the majority of NP O_2 probes are high specific brightness, photostability, relative ease of fabrication and up-scaling. The challenges are the significant size (usually >40 nm, i.e. larger than the other probes), fabrication processes to achieve reproducible composition and structure, stability under prolonged storage (drying and sterilization can be problematic), biocompatibility and toxicity in in vivo applications.

Endogenous O_2-sensitive probes are comprised of the photoluminescent structures which are encoded genetically and/or produced in living cells. A well-known approach is the imaging of respiration activity of cells by ratiometric analysis of fluorescent electron donors and redox indicators NADH and FAD [73]. The advantage is that these indicators are present in all cell lines; however, they possess low quantum yields of fluorescence (<1%) and require intense illumination of the sample. Protoporphyrin IX is another important fluorescent intermediate involved in heme biosynthesis. It can be overproduced in cells in the presence of increased amounts of 5-aminolevulinic acid

(ALA) and used as an O$_2$ probe by measuring its delayed fluorescence [74]. This methodology has been tested with cultured cells, isolated hepatocytes and in vivo with intact hearts [26, 74, 75]. At the same time, the limitations of this probe are the low yield of delayed fluorescence along with strong short-lived fluorescence in the same spectral region, rather low photostability and photosensitisation activity of protoporphyrin IX. For the fluorescent redox indicators and other endogenous probes, including NAD(P)H and FAD, there are good opportunities for multiplexing with the phosphorescent probes; however, such studies are still rather scarce [74, 76, 77].

Some fluorescent proteins of GFP family produce an O$_2$-dependent red shift in fluorescence upon their photo-activation with blue light [25]. Although this process only occurs at around 0–2% O$_2$, this methodology was applied successfully to study iO$_2$ gradients in Hep3b cells with mitochondria-targeted GFP [78].

For effective use in physiological experiments with complex biological samples, possible toxic effects of the selected O$_2$ probe on the cells, conditions, working concentration and time of use must be assessed and optimised at the start. For simple biological models, such as cell cultures or tissue slices, effects on cell viability, proliferation, energy production pathways and mitochondrial function are usually examined [5, 74]. For in vivo applications [3], factors such as systemic and organ toxicity (e.g. kidney, liver), probe distribution, metabolism and clearance of its components should be considered.

Measurement modalities

The main detection modalities in O$_2$ sensing are: (1) *intensity* measurements at a single wavelength; (2) *ratiometric intensity* measurements with a reference (O$_2$-insensitive) dye; and (3) *lifetime based sensing* by phase modulation technique [29, 79] or by time-gated fluorometry under pulsed excitation. Since emission lifetimes of phosphorescent O$_2$ probes lie in the microsecond range, implementation of lifetime-based O$_2$ sensing is technically more easy than for conventional (nanosecond) probes and luminophores [29, 80].

Simple photoluminescence intensity measurements are generally prone to optical interferences, especially by complex biological samples producing high light scattering and autofluorescence that may affect probe calibration and lead to incorrect O$_2$ readings. Phase fluorometry can also be affected by these factors, unless special signal processing algorithms are applied (see, e.g., [52]). *Time-resolved fluorometry* (TR-F) in the microsecond time domain allows better signal-to-noise ratio and more reliable and accurate O$_2$ quantification via measurement of

probe emission decay [3, 81]. In a simplified format called rapid lifetime determination (RLD) [80, 82], emission intensity signals (F_1, F_2) are collected at two different delay times (t_1, t_2) after the excitation pulse, from which lifetime is calculated as:

$$\tau = (t_2 - t_1) / \ln(F_1/F_2) \tag{3}$$

A number of commercial instruments—multi-label readers originally developed for sensitive detection of lanthanide chelate labels—have TR-F and RLD capabilities and can operate with existing O$_2$ probes on different assay substrates (96- and 384-well plates) [57]. One should keep in mind that such instruments have PMT detectors which are usually insensitive above 700 nm (or even above 650 nm), and their time resolution is limited by the Xe-flashlamp used (pulse width of $\geq$20 μs). Furthermore, instrument sensitivity, signal-to-noise ratio, accuracy of lifetime determination, temperature control of the sample and software capabilities may vary greatly depending on the make and model. Having tested many different instruments and probes, we consider Victor® (PerkinElmer, Finland) and FLUOstarOmega™ (BMG, Germany) TR-F reader families among the best in terms of their sensitivity and selectivity of probe detection (S/N ratio >100), accuracy and resolution in RLD mode and temperature control. These instruments work well with PtCP and PtPFPP based probes including MitoXpress™, peptide conjugates and nanoparticles, and are now used in the high-throughput assessment of O$_2$ in cell populations and other sample types [57, 60, 83–86]. Representative profiles of respiration and cellular O$_2$ generated using both extracellular and intracellular O$_2$ sensing probes are shown in Fig. 1. Many standard instruments are not very compatible with the short-decay emitting probes based on Ru(II) complexes and/or with the longwave O$_2$ probes emitting in the very-near infrared. On the other hand, custom-built instruments tailored to the particular O$_2$-sensitive probes demonstrate good performance in O$_2$ measurement [31, 80].

Besides the macroscopic, or 'cuvette' formats, the above detection modalities can also be integrated with *live cell/tissue imaging* (LCI) platforms to implement *O$_2$ imaging*. Thus, relatively simple and inexpensive wide-field fluorescence microscopes allow two-dimensional (2-D) visualisation with sub-cellular spatial resolution of respiring objects loaded with an O$_2$ probe. Using conventional intensity-based mode, standard LCI systems allow monitoring of relative changes in cell oxygenation and respiration activity over time. With a proper calibration (e.g. measuring probe signal at several known pO$_2$ levels), fluorescence intensity images can be converted into [O$_2$] maps [81]. However, intensity calibrations are rather unstable due to significant probe photobleaching and signal drift under illumination (which should be minimised by all
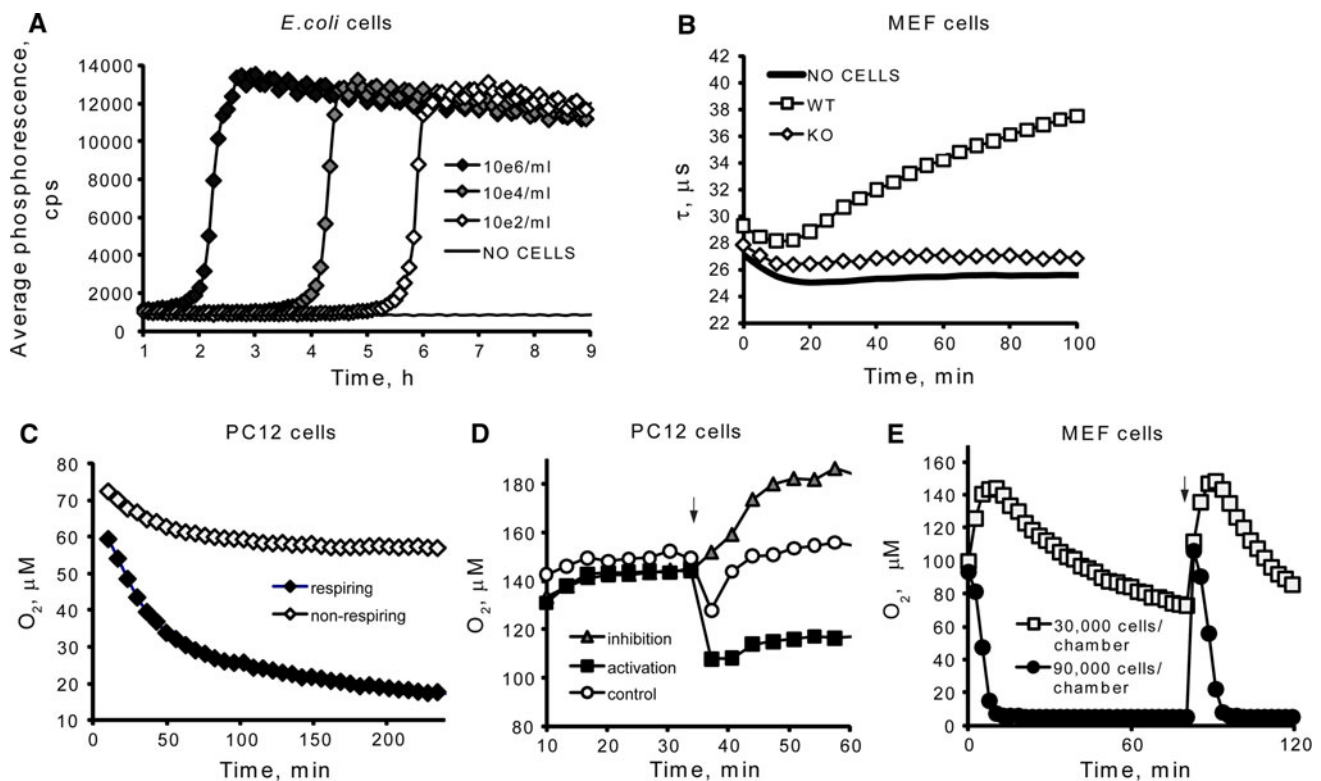
Fig. 1 Different signal profiles revealed with the O_2 sensing probes. **a** Microbial respiration/growth of *E. coli* measured in phosphorescence intensity mode. The number of cells in the original sample (cfu/g) is determined from the time required to reach signal threshold [121]. **b** Respiration profiles of eukaryotic cells measured in RLD mode: wild-type (*WT*) mouse embryonic fibroblasts, knock-out (*KO*) cells deficient with Krebs cycle enzyme and blank control. OCRs are calculated from the slope of probe signal [57]. **c** Profiles of oxygenation for the respiring and non-respiring PC12 cells under mild atmospheric hypoxia (8% pO_2). **d** Changes in icO_2 in respiring PC12 cells upon the addition of uncoupler (FCCP), inhibitor (AntA) and mock control (DMSO), at 20.9% pO_2. *Arrow* indicates the time of effector addition. **e** Oxygenation of MEF cells grown at different densities in a microfluidic chip Ibidi®, measured under static conditions. Flushing the chamber with fresh medium (at the start and at *arrow*) causes reoxygenation and subsequent deoxygenation of the cells. **a**, **b** were generated with ecO_2 probe MitoXpress™ [80]; **c–e** with pre-calibrated icO_2 probes [61, 71]

means), and affected by sample distortion (manipulation with cells or effector addition). Using a more complex probe with two reporter dyes (1 is O_2-insensitive) and ratiometric intensity imaging mode [69, 70], it is possible to stabilise the O_2 calibration if the two dyes photobleach at approximately the same rate. For high-resolution O_2 imaging, probe photostability becomes one of the main selection criteria and many current probes are not quite optimal in this regard. In addition, many O_2-sensitive dyes are effective sensitisers of singlet oxygen production [87]. Their use in imaging experiments needs thorough optimisation to ensure sufficiently high, reliably measurable luminescent signals and low phototoxicity and cell damage [30, 53].

Laser-scanning microscopy, represented by confocal and multi-photon luminescence LCI systems, allow visualisation of complex objects with sub-micron spatial resolution, and generation of corresponding O_2 maps in 3-D and 4-D (in time-lapse experiments) [87]. Multi-photon systems, which employ high-power NIR lasers, provide

deeper tissue penetration (several hundred microns) and better spatial resolution; however, they are currently expensive, require indicator dyes with large cross-section of two-photon absorption and special tuning of hardware and software for the measurement of long-decay emission of O_2 probes. A number of dedicated O_2 probes with two-photon and FRET antennae, imaging systems and applications on their basis have been described recently [77, 88–92], and this area continues to develop rapidly.

Phosphorescence and fluorescence lifetime imaging microscopy (FLIM) enables visualisation of O_2 distribution in complex biological samples, and accurate quantification of O_2. On a microscope with wide-field illumination, 2-D O_2 imaging can be realised using pulsed excitation with a suitable LED or laser delivering trains of ns-µs pulses at kHz frequency, and gated CCD camera operating in the microsecond time range [81]. Following each excitation pulse and a time delay (variable), emitted photons are collected by the camera over the measurement window time and integrated over a number of pulses to generate an

intensity frame. This is repeated at several delay times, and from these frames emission decay is reconstructed and lifetime is determined for each pixel of the CCD matrix. By applying a probe calibration function (determined in a separate experiment), lifetime images of the sample can be converted into an O$_2$ concentration map. For the laser-scanning systems, emission lifetimes are measured sequentially for each pixel with a PMT or photodiode detector, processed by the software to generate 2-D images of Z-stacks which are then assembled together.

Many existing O$_2$ probes are spectrally compatible with modern LCI systems which usually contain several light sources (lamps, LEDs, lasers) and detectors (red-NIR sensitive PMTs, photodiodes or CCD cameras). One should keep in mind that off-the-shelf LCI systems are designed to operate in intensity and ratiometric (multi-colour) modes and with nanosecond fluorophores. They have to be custom-tuned for use with long-decay emitting O$_2$ probes, preferably upgraded to support FLIM mode and calibrated carefully for quantitative O$_2$ imaging [91, 93]. Due to long-decay emission of the O$_2$ probe, generation of detailed 2-D and 3-D O$_2$ maps on FLIM systems requires relatively long signal acquisition time. So, even for the very sophisticated custom-built O$_2$ imaging systems, temporal resolution is not as good as for the imaging systems operating with nanosecond probes. Different LCI and FLIM systems have different signal acquisition settings, so that several key parameters require basic optimisation for each particular O$_2$ probe and application.

A number of alternative, specialised techniques have been described recently, which are not discussed here; for example, non-radiative triplet quenching of the lumino-phores under high-power pulsed laser excitation [26] and photoacoustic sensing [94].

Probe localisation and measurement formats

Depending on the measurement task, the O$_2$ probe needs to be introduced in a particular compartment of the sample, cell or tissue, or applied to measure a particular pool of sample O$_2$ such as extracellular or intracellular (see Table 2).

For imaging of tissue O$_2$, *extracellular, cell-impermeable* probes are usually employed, which are injected into blood stream or bulk tissue. Such a probe is expected to stay in the vasculature without penetrating the cells, and to have low cyto- and organ toxicity (e.g. kidney or liver damage), especially in prolonged in vivo experiments [91]. For the measurement of OCR, and related in vitro applications with cultured cells, extracellular probes dissolved in the medium are used [57] (solid-state O$_2$ sensitive coatings may also be suitable for these applications [50]).

Intracellular probes

In some applications and measurement tasks, it is necessary to introduce the probe directly into the cell and maintain it inside during the measurement without damaging the cell or affecting its normal function. Cell loading is relatively easy to achieve with phagocytic cells (e.g. macrophages [69]) using particle-based probes; however, loading of the majority of other cells is more challenging. Facilitated transport systems, such as microinjection, electroporation [66], facilitated endocytosis [80, 93], liposomal transfer and gene gun [95], have been used with some success, but these techniques require additional reagents/steps, and are tedious, invasive and stressful for the cells. They rarely provide high and/or uniform loading of cell populations, and show a high degree of cell specificity, with dependence on the conditions used (medium, additives, temperature, cell type). These techniques are difficult to use routinely.

A more efficient strategy for cell loading is to develop O$_2$ probes with cell-penetrating ability [42, 60–62] or to introduce 'delivery vectors' in existing probe structures [65]. This has been demonstrated with several supramolecular- and nanoparticle-based probes, for which fast (6–16 h) and efficient cell loading comparable with the delivery of conventional small molecule cargo or cell transfection with genetically-encoded biosensor probes [25, 96] was achieved. A significant degree of cell specificity can still be seen as no universal cell-loading vector currently exists [63]. Rational design potentially allows for targeted delivery of an O$_2$ probe to a particular location within the cell, by altering molecular charge or peripheral groups, or by incorporating special functionality and additional 'vectors' responsible for the delivery of the cargo (e.g. mitochondria targeting peptide sequences [97]). As with many other probes and drugs, a well-defined intracellular localisation is desirable. However, this is not so critical for the O$_2$ probes because O$_2$ is not contained in a specific location within the cell and diffuses quickly across and through the biological membranes. Phototoxicity and cell damage depend on the location of the probe within the cell. For example, photosensitisers of porphyrin origin used in photodynamic therapy of cancer show maximal photodamage when they are targeted to cell membranes or the nuclei [98, 99]. Based on this, one can predict [87] that for O$_2$ sensing the probe should be targeted to a different part of the cell, for example to the cytoplasm.

Applications and biological uses

Common phosphorescence based O$_2$-sensitive probes and their biological applications are summarised in Table 2.

Table 2 An overview of O_2 sensing probes tested in biological applications

Probe name and type	Application, probe location	Equipment, detection mode	K_{s-v}, μM^{-1}/ τ_0, μs	Status, comments	Refs.
Extracellular probes					
PdTPCPP (conjugated to BSA) SM	O_2 mapping in tissues. Probe in blood/vasculature	Ex 416, 523 nm. Em 690 nm. Scanning phosphorescence quenching microscopy	0.382/~700	Quantitative. Point measurement. Used by several labs	[54, 101–106]
Oxyphor R2 (PdTPCPP dendrimer) SM	O_2 mapping in tissues. Probe in blood/vasculature	Phase fluorometry: Ex 524 nm, Em 690 nm, 4 mm light guide; Two-photon microscope	0.343/640 (38°C, pH 7.4)	Quantitative. Point measurement. Used by several labs	[31, 105]
Oxyphor G2 (PdTCPTBP dendrimer) SM	Tissue O_2 gradients in vivo. Probe in blood/vasculature	Wide field FLIM: Ex 440/632 nm, Em 790 nm	0.086/251 (38°C, pH 7.4)	Quantitative. Used by several labs and with different models. Validated	[31, 106]
MitoXpress (PtCP conjugate) SM	OCR by cells, mitochondria, enzymes. Assessment of cell bioenergetics. Probe added to the medium	TR-F reader, RLD: Ex 340–420 nm, Em 640–660 nm	~0.011/80	Quantitative. Used by many labs. Validated in drug screening	[19, 33, 57, 107]
PtP-C343 (PtTAOP-Coumarin 343 dendrimer) SM	Tissue O_2. In vivo O_2 gradients. Probe in blood/vasculature	Two-photon FLIM: Ex 840 nm, Em 682 nm	>0.11/60	Quantitative. Require special equipment and set-up. Used in several labs	[91, 93, 108]
Oxyphors R4 and G4	Tissue O_2 gradients in vivo. Tumor imaging. EC probe in blood/vasculature/interstitial space	Wide-field FLIM Ex 428, 530 nm (R4); 448, 637 (G4) Em 698 (R4), 813 (G4)	R4: 0.098/681 (37°C, pH 7.2) G4: 0.083/218 (38.2°C, pH 7.2)	Quantitative. Require special equipment and set-up	[109]
PS-NP (polystyrene NP doped with PdTPTBP and DY635, reference)	Targeted tumor in vivo imaging. EC probe	Ratiometric-based. Lifetime-based. Ex 635 nm. Em 670 nm (reference); 800 nm (O_2 sensitive)	ND	Quantitative. May be used for intracellular measurement with modified coating	[72]
Intracellular probes					
O_2 PEBBLEs (PtOEPK and OEP, ormosil) NP	Cell oxygenation. Impermeable probe loaded with gene gun	Ratiometric wide field imaging. Ex 568 nm, Em 620/750 nm	0.032/NA	Semi-quantitative (relative). Stressful loading. 1 cell type tested	[95]

Table 2 continued

Probe name and type	Application, probe location	Equipment, detection mode	K_{s-v}, μM^{-1}/ τ_0, μs	Status, comments	Refs.
MitoXpress (PtCP conjugate), SM	Cell oxygenation Metabolic responses Impermeable probe loaded with Endo-Porter	TR-F reader, RLD: Ex 340–420 nm Em 640–660 nm	~0.006/70	Quantitative. Facilitated loading required (16 h); 6 cell types tested (cell-specific)	[80, 83–86]
Ru(II)-(py)$_3$-R$_8$ (peptide conjugate). SM	O2 mapping in cells Cell-permeable, self-loading probe	Wide field FLIM: Ex 460 nm Em 607 nm	ND	Semi-quantitative. 1 cell type tested	[42]
Cell penetrating PtCP peptide conjugates: PEPP0, 3, PtCPTE-CFR$_8$, SM	Cell oxygenation, Metabolic responses Cell-permeable, self-loading probe	TR-F reader, RLD: Ex 340–420 nm Em 640–660 nm Intravital confocal imaging was also demonstrated	~0.006/70	Quantitative. >6 cell lines tested Controlled sub-cellular location	[60–62, 110]
PtOEP/PDHF and PFO–NP	O$_2$ mapping in cells Probe uptake by macrophages	Ratiometric wide field imaging: Ex 350 nm Em 440/650 nm	ND	Semi-quantitative. One cell line tested (macrophages). Particle variability, require UV excitation	[69]
Near infrared PAA NPs (Oxyphor G2 probe in PAA gel, with peptide coat) NP	Cell oxygenation Cell permeable, self-loading probe	Wide field and confocal imaging: Ex 633 nm Em 790 nm	0.034/ND (37°C) (without cells)	Quantitative. Several cell lines tested. High probe concentrations used. Cross-sensitivity to pH	[65]
RGB NPs (PtTFPP and BCPN in aminated polystyrene) NP	Cell oxygenation Cell permeable, self-loading probe	Wide-field RGB imaging: Ex 330–380 nm Em Red, Green	~0.0083/NA	Semi-quantitative. 1 cell line tested. NP variability, long loading 48 h	[70]
NANO2 (PtPFPP in RL100 polymer) NP	Cell oxygenation Metabolic responses, cell bioenergetics Cell permeable, self-loading probe	TR-F reader: RLD Ex 340–420 nm Em 640–660 nm Wide-field FLIM and confocal O$_2$ imaging	~0.006/67	Quantitative. >5 cell lines tested. High brightness and photostability	[71]

K_{s-v} constants were calculated based on published data with assumption that at normal atmospheric pressure O$_2$ has 160 mmHg with dissolved concentration ~200 μM or 4,950 ppm

PAA polyacrylamide hydrogel, *PDHF* poly(9,9-dihexylfluorene), *PFO* poly(9,9-dioctylfluorene), *SM* supramolecular, *NA* not applicable, *ND* no data reported, *NP* nanoparticle-based, *BCPN* butyl-N-(5-carboxypentyl)-4-piperidino-1,8-naphtalimide

Average OCR or O₂ concentration can be measured using an extracellular O_2 probe added to the sample. Such measurements can be conducted in cuvettes or microplates on a conventional fluorescent spectrometer or TR-F reader [5, 19]. To measure absolute OCR values, a sealed, gas-impermeable vessel should be used [58]. If the sample is heterogeneous and contains precipitating matter (e.g. suspension of cells), stirring should be provided to eliminate the formation of local O_2 gradients which may lead to incorrect results. To assess relative OCRs (e.g. treated vs. untreated cells), the set-up can be simplified, for example using standard microtiter plates, which facilitate cell growth, liquid handling and up-scaling, and partial sealing of samples with mineral oil added to the wells prior to the measurement [58]. The oil forms a barrier for ambient O_2 diffusion, and leads to the development of an O_2 gradient in the sample which can be monitored with the O_2 probe and related to the OCR [57, 84]. This is a convenient format for analysing large number of samples of similar type, e.g. when screening compound libraries for mitochondrial and cytotoxicity, or analysing panels of transformed cells or microbial cultures. Simple fluorescence intensity measurements can be used in these applications, with proper controls for possible optical interferences and measurement artefacts [19]. Representative respiration profiles of bacterial and mammalian cells are shown in Fig. 1a, b.

In vivo O₂ imaging is of high fundamental and practical importance. Measurement of actual oxygenation in live respiring tissue (e.g. brain or muscle), localised O_2 gradients in the vasculature (blood vessels, capillaries) or tumour oxygenation can be realised using extracellular O_2 probes and phosphorescence lifetime-based O_2 imaging [106, 111–113]. This was also realised with a fibre-optic probe and point-by-point measurements [54], and in plant cells [79]. In recent years, wide-field FLIM systems and high-resolution confocal and two-photon laser-scanning systems [114] for imaging tissue O_2 were successfully used in complex in vivo and ex vivo studies.

Thus, a new dendrimeric probe with coumarin antennae, for which a detailed synthesis protocol was published [115], was applied to measure local oxygenation in rodent brain on a custom-built two-photon FLIM LCI system [91]. The cell-impermeable PtP-C343 probe was injected into the blood stream and measured in the brain tissue at different distances from arterial regions [31, 93]. This system showed a spatial resolution of 100 μm, stable O_2 calibration practically unaffected by the environment, and probe retention in the body (half-life) of about 2 h.

Other in vivo studies include: O_2 mapping of rodent retina where the application of anaesthetics was shown to decrease venous O_2 tension [54, 106]; O_2 dynamics in individual frog skeletal muscle fibres showing that faster frequency of muscle stimulation leads to higher drops in pO_2 in adaptive manner [116]; measurement of pO_2 in microcirculation [100, 101], tumour oxygenation [56, 72]; and FLIM of cortical extravascular O_2 in the ischemia–reperfusion model [91];

The development of icO_2 probes has extended the capabilities of O_2 sensing, particularly with respect to the *in situ oxygenation* of respiring samples. Thus, adherent cells in their native differentiated state can be analysed in open microplates or sealed samples (perfusion cell or culture flask). In such assays, the main parameters that require control and optimisation are cell density and metabolic activity, diffusion and mass exchange characteristics of the sample (volume of medium, viscosity, temperature) and external pO_2 [84]. icO_2 probes can be used in conjunction with TR-F readers (described above) providing simplicity, convenience, high sample throughput and good analytical performance. This sensing methodology has been applied to monitor changes in cell respiration and metabolism, responses of cells to stimulation with effectors (with treatment applied during the measurement) and to hypoxia [80, 84]. It has been used in several mechanistic studies with complex biological models [83, 85, 86]. Representative profiles of icO_2 produced with mammalian cells are shown in Fig. 1c–e.

The icO_2 probes were also used in microscopy imaging formats, to perform semi-quantitative intensity-based assessment of cellular O_2 or more accurate measurement by FLIM [81]. For example, they were used in in situ respirometry with skeletal muscles [53, 102, 116], and in ex vivo imaging experiments with carotid body where cell oxygenation was correlated with the other parameters of cellular function [110]. Furthermore, perfusion chambers, microfluidic devices and 3-D tissue cultures are becoming increasingly popular in biological experiments [117]. For such systems, reliable control of sample oxygenation is critical, and it can be implemented by means of icO_2 probes and contactless measurements. And in OCR measurements with adherent cells and tissue under non-stirring conditions (e.g. on a microplate under oil), icO_2 probes can provide better sensitivity than conventional extracellular probes.

Finally, one can consider combining different O_2-sensing probes and techniques to control O_2 in complex biological experiments, for example in cell culture, tissue engineering, or experiments under hypoxic environment. Examples of such tools and measurement set-ups shown in Fig. 2 include: (1) a hypoxia chamber (macro-system) which can be set at different pO_2 levels; (2) solid-sate O_2 sensors placed inside the chamber at different locations; (3) a handheld optical scanner which interrogates with the sensors (from outside or inside the chamber) and reads current O_2 concentration; (4) a tissue culture flask (mini-system) with built-in sensor spots also measurable with the
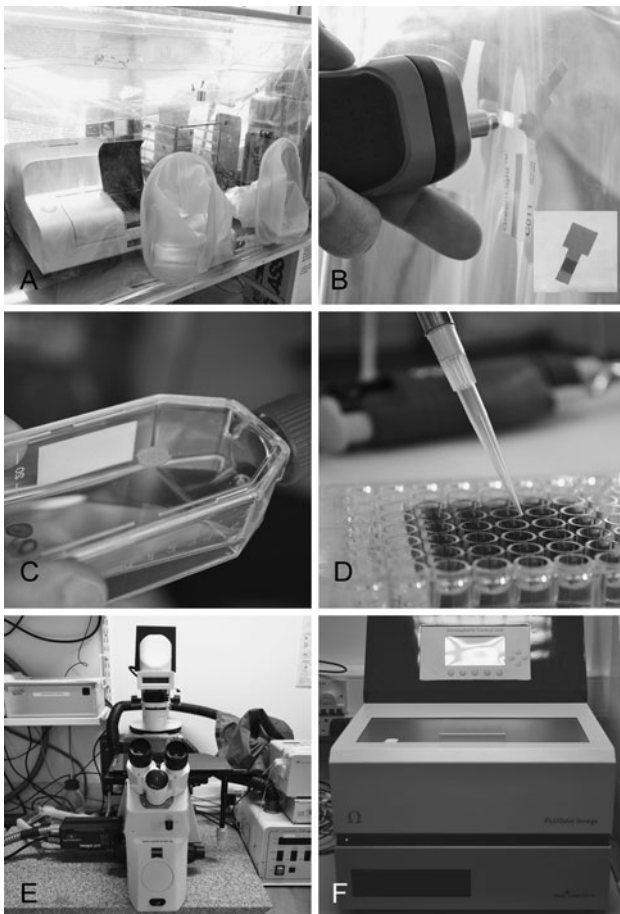
Fig. 2 Hypoxia workstation with optical O$_2$ probes and sensors. **a** Glove-box with controlled atmosphere (adjustable O$_2$), temperature and humidity, in which cultured cells, accessories and measurement equipment are placed. **b** Solid-state O$_2$ sensors placed inside the glove box are read with a hand-held scanner from the outside. **c** Tissue culture flask with built-in O$_2$ sensor dot that can also be measured with the scanner. **d** Microplate with cultured cells to which an O$_2$-sensing probe is added. **e** Live cell O$_2$-imaging system—fluorescent microscope with FLIM capabilities. **f** TR-F microplate reader which can read the IC and EC probes and measure OCR and icO$_2$ in a microplate with respiring samples; this instrument is also equipped with O$_2$/CO$_2$ control of microplate compartment

handheld scanner; (5) a microplate containing cells together with an intracellular or extracellular O$_2$ probe (microsystem); (6) a TR-F reader which can read the microplate and monitor oxygenation and respiratory responses in cell populations; and (7) an imaging system which can perform detailed analysis of individual cells, cell populations and live tissue with high spatial resolution (nano-system).

Conclusions and future prospects

Overall, a fairly broad variety of different O$_2$ sensing probes, measurement formats and applications have been described and tested, and each of them possesses merits

and limitations. To ensure proper selection and use for a particular biological model or measurement task, it is necessary to demonstrate their analytical performance under relevant experimental conditions, determine structure–function relationships and work out detailed operational protocols that can be easily adopted by ordinary (non-skilled) users. Thus far, only some of these probes and techniques (see Table 2) have been shown to provide quantitative and reproducible measurement of O$_2$ with stable and accurate calibrations. Many others have stuck at the stage of proof of concept, with incomplete optimisation, unsatisfactory working specifications and analytical performance, and semi-quantitative or qualitative data output (relative changes in O$_2$ concentration or use under 'clean' conditions). This limits their adoption by the broad community of biomedical researchers. Another practical issue is the low level of understanding by the end-user of the basic principles underlying each particular O$_2$-sensing technique and defining the scope of its applicability. This often leads to negative results in first experiments and dissatisfaction with the method which is then difficult to overcome. To make a way towards wider practical use, these probes and techniques, which exist in many variations outlined above, require substantial development and improvement, comprehensive validation in biological experiments and demonstration in cutting-edge physiological studies.

On the application side, initial bioenergetic, metabolic, cell biology and toxicological studies using O$_2$-sensing techniques have been applied to rather simple, macroscopic samples, such as mitochondrial preparations [118], suspension cell lines [57] and perfused respiring tissue [24]. Nowadays, the focus is shifting towards more complex models and real-life systems: adherent differentiated cells [83–86], ex vivo and in vivo systems, such as intact respiring brain, muscle, tumour tissue and vasculature [90, 91]. More recently, detailed mapping and reconstruction of O$_2$ gradients on a micro-scale and in 3-D have been demonstrated in tissue and even in individual cells [26, 81], which require thorough verification. New 'super-resolution' imaging platforms are now emerging [119]; however, their usability with the long-decay O$_2$ probes has still to be demonstrated.

Measurement of local O$_2$ concentrations and gradients in tissues and within the cell is important for research areas such as cancer metabolism, neuroscience, effects of hypoxia on cell physiology, biomedical devices and wound healing. For macro-objects, such as tissue slices, organs or whole organisms, O$_2$ is also a valuable parameter, for example in radio- and chemotherapy, assisted reproductive technology and organ transplantation [120]. The demand for non-invasive O$_2$ measurement systems spans well beyond the above mentioned areas and models. It is also

highly relevant for biotechnology, environmental monitoring, food, and chemical and industrial process control.

References

1. Semenza GL (2007) Life with oxygen. Science 318(5847):62–64
2. Wilson DF (2008) Quantifying the role of oxygen pressure in tissue function. Am J Physiol Heart Circ Physiol 294(1):H11–H13. doi:10.1152/ajpheart.01293.2007
3. Wilson DF, Finikova OS, Lebedev AY, Apreleva S, Pastuszko A, Lee WMF, Vinogradov SA (2011) Measuring oxygen in living tissue: intravascular, interstitial, and "Tissue" oxygen measurements. In: Oxygen Transport to Tissue XXXII, vol 701. Advances in Experimental Medicine and Biology. Springer, US, pp 53–59. doi:10.1007/978-1-4419-7756-4_8
4. Semenza GL (2007) Oxygen-dependent regulation of mitochondrial respiration by hypoxia-inducible factor 1. Biochem J 405(1):1–9
5. Brand MD, Nicholls DG (2011) Assessing mitochondrial dysfunction in cells. Biochem J 435(2):297–312. doi:10.1042/bj20110162
6. Lin J, Handschin C, Spiegelman BM (2005) Metabolic control through the PGC-1 family of transcription coactivators. Cell Metab 1(6):361–370
7. Bartrons R, Caro J (2007) Hypoxia, glucose metabolism and the Warburg's effect. J Bioenerg Biomembr 39(3):223–229
8. Clark LC, Wolf R, Granger D, Taylor Z (1953) Continuous recording of blood oxygen tensions by polarography. J Appl Physiol 6(3):189–193
9. Wittenberg JB (1970) Myoglobin-facilitated oxygen diffusion: role of myoglobin in oxygen entry into muscle. Physiol Rev 50(4):559–636
10. Sullivan SM, Pittman RN (1984) In vitro O2 uptake and histochemical fiber type of resting hamster muscles. J Appl Physiol 57(1):246–253
11. Williams BB, Khan N, Zaki B, Hartford A, Ernstoff MS, Swartz HM (2010) Clinical Electron Paramagnetic Resonance (EPR) oximetry using India ink. In: Oxygen transport to tissue XXXI, vol 662. Advances in experimental medicine and biology. Springer, US, pp 149–156. doi:10.1007/978-1-4419-1241-1_21
12. Cringle SJ, Yu PK, Su EN, Yu DY (2006) Oxygen distribution and consumption in the developing rat retina. Invest Ophthalmol Vis Sci 47(9):4072–4076
13. Braun RD, Lanzen JL, Snyder SA, Dewhirst MW (2001) Comparison of tumor and normal tissue oxygen tension measurements using OxyLite or microelectrodes in rodents. Am J Physiol Heart Circ Physiol 280(6):H2533–H2544
14. Dewhirst MW, Secomb TW, Ong ET, Hsu R, Gross JF (1994) Determination of local oxygen consumption rates in tumors. Cancer Res 54(13):3333–3336
15. Wu C-C, Luk H-N, Lin Y-TT, Yuan C-Y (2010) A Clark-type oxygen chip for in situ estimation of the respiratory activity of adhering cells. Talanta 81(1–2):228–234
16. Yadava N, Nicholls DG (2007) Spare respiratory capacity rather than oxidative stress regulates glutamate excitotoxicity after partial respiratory inhibition of mitochondrial complex I with rotenone. J Neurosci 27(27):7310–7317. doi:10.1523/jneurosci.0212-07.2007
17. Liu Y, Villamena FA, Sun J, Wang T-y, Zweier JL (2009) Esterified trityl radicals as intracellular oxygen probes. Free Radic Biol Med 46(7):876–883
18. Bobko AA, Dhimitruka I, Eubank TD, Marsh CB, Zweier JL, Khramtsov VV (2009) Trityl-based EPR probe with enhanced sensitivity to oxygen. Free Radic Biol Med 47(5):654–658
19. Diepart C, Verrax J, Calderon PB, Feron O, Jordan BF, Gallez B (2010) Comparison of methods for measuring oxygen consumption in tumor cells in vitro. Anal Biochem 396(2):250–256
20. Halevy R, Shtirberg L, Shklyar M, Blank A (2010) Electron spin resonance micro-imaging of live species for oxygen mapping. J Vis Exp (42):e2122
21. Rosenberger C, Rosen S, Paliege A, Heyman SN (2009) Pimonidazole adduct immunohistochemistry in the rat kidney: detection of tissue hypoxia. Methods Mol Biol 466:161–174. doi:10.1007/978-1-59745-352-3_12
22. Liu Q, Vo-Dinh T (2009) Spectral filtering modulation method for estimation of hemoglobin concentration and oxygenation based on a single fluorescence emission spectrum in tissue phantoms. Med Phys 36(10):4819–4829
23. Chang J, Wen B, Kazanzides P, Zanzonico P, Finn RD, Fichtinger G, Ling CC (2009) A robotic system for 18F-FMISO PET-guided intratumoral pO2 measurements. Med Phys 36(11):5301–5309
24. Rumsey WL, Vanderkooi JM, Wilson DF (1988) Imaging of phosphorescence: a novel method for measuring oxygen distribution in perfused tissue. Science 241(4873):1649–1651. doi:10.1126/science.3420417
25. Takahashi E, Takano T, Nomura Y, Okano S, Nakajima O, Sato M (2006) In vivo oxygen imaging using green fluorescent protein. Am J Physiol Cell Physiol 291(4):C781–C787. doi:10.1152/ajpcell.00067.2006
26. Mik EG, Johannes T, Zuurbier CJ, Heinen A, Houben-Weerts JHPM, Balestra GM, Stap J, Beek JF, Ince C (2008) In vivo mitochondrial oxygen tension measured by a delayed fluorescence lifetime technique. Biophys J 95(8):3977–3990
27. Stern O, Volmer M (1919) The fading time of fluorescence. Phys Z 20:183–188
28. Carraway ER, Demas JN, DeGraff BA, Bacon JR (1991) Photophysics and photochemistry of oxygen sensors based on luminescent transition-metal complexes. Anal Chem 63(4):337–342. doi:10.1021/ac00004a007
29. Papkovsky DB (2004) Methods in optical oxygen sensing: protocols and critical analyses. Methods Enzymol 381:715–735. doi:10.1016/S0076-6879(04)81046-2
30. Schweitzer C, Schmidt R (2003) Physical mechanisms of generation and deactivation of singlet oxygen. Chem Rev 103(5):1685–1758. doi:10.1021/cr010371d
31. Dunphy I, Vinogradov SA, Wilson DF (2002) Oxyphor R2 and G2: phosphors for measuring oxygen by oxygen-dependent quenching of phosphorescence. Anal Biochem 310(2):191–198
32. Papkovsky DB, O'Riordan TC (2005) Emerging applications of phosphorescent metalloporphyrins. J Fluoresc 15(4):569–584. doi:10.1007/s10895-005-2830-x
33. Hynes J, Floyd S, Soini AE, O'Connor R, Papkovsky DB (2003) Fluorescence-based cell viability screening assays using water-soluble oxygen probes. J Biomol Screen 8(3):264–272. doi:10.1177/1087057103008003004
34. Borisov SM, Nuss G, Klimant I (2008) Red light-excitable oxygen sensing materials based on platinum(II) and palladium(II) benzoporphyrins. Anal Chem 80(24):9435–9442. doi:10.1021/ac801521v

35. Lebedev AY, Cheprakov AV, Sakadzic S, Boas DA, Wilson DF, Vinogradov SA (2009) Dendritic phosphorescent probes for oxygen imaging in biological systems. ACS Appl Mater Interfaces 1(6):1292–1304. doi:10.1021/am9001698

36. O'Riordan TC, Fitzgerald K, Ponomarev GV, Mackrill J, Hynes J, Taylor C, Papkovsky DB (2007) Sensing intracellular oxygen using near-infrared phosphorescent probes and live-cell fluorescence imaging. Am J Physiol Regul Integr Comp Physiol 292(4):R1613–R1620. doi:10.1152/ajpregu.00707.2006

37. Thomas PC, Halter M, Tona A, Raghavan SR, Plant AL, Forry SP (2009) A noninvasive thin film sensor for monitoring oxygen tension during in vitro cell culture. Anal Chem 81(22):9239–9246. doi:10.1021/ac9013379

38. Kadish KM, Smith KM, Guilard R (2010) Handbook of porphyrin science, V.4. Phototherapy, radioimmunotherapy and imaging, vol 4. World Scientific, Singapore

39. Sharman WM, van Lier JE, Allen CM (2004) Targeted photodynamic therapy via receptor mediated delivery systems. Adv Drug Deliv Rev 56(1):53–76

40. O'Connor AE, Gallagher WM, Byrne AT (2009) Porphyrin and nonporphyrin photosensitizers in oncology: preclinical and clinical advances in photodynamic therapy. Photochem Photobiol 85(5):1053–1074. doi:10.1111/j.1751-1097.2009.00585.x

41. Mitra S, Foster TH (2000) Photochemical oxygen consumption sensitized by a porphyrin phosphorescent probe in two model systems. Biophys J 78(5):2597–2605. doi:10.1016/S0006-3495(00)76804-4

42. Neugebauer U, Pellegrin Y, Devocelle M, Forster RJ, Signac W, Moran N, Keyes TE (2008) Ruthenium polypyridyl peptide conjugates: membrane permeable probes for cellular imaging. Chem Commun 42:5307–5309

43. Geddes CD, Lakowicz JR, DeGraff BA, Demas JN (2005) Luminescence-based oxygen sensors. In: Geddes CD (ed) Reviews in fluorescence 2005, vol 2005. Springer, US, pp 125–151. doi:10.1007/0-387-23690-2_6

44. Zitova A, Hynes J, Kollar J, Borisov SM, Klimant I, Papkovsky DB (2010) Analysis of activity and inhibition of oxygen-dependent enzymes by optical respirometry on the LightCycler system. Anal Biochem 397(2):144–151

45. Borisov SM, Klimant I (2007) Ultrabright oxygen optodes based on cyclometalated iridium(III) coumarin complexes. Anal Chem 79(19):7501–7509. doi:10.1021/ac0710836

46. O'Riordan TC, Soini AE, Soini JT, Papkovsky DB (2002) Performance evaluation of the phosphorescent porphyrin label: solid-phase immunoassay of alpha-fetoprotein. Anal Chem 74(22):5845–5850

47. Finikova OS, Cheprakov AV, Vinogradov SA (2005) Synthesis and luminescence of soluble meso-unsubstituted tetrabenzo- and tetranaphtho[2,3]porphyrins. J Org Chem 70(23):9562–9572. doi:10.1021/jo051580r

48. Lakowicz J, Terpetschnig E, Murtaza Z, Szmacinski H (1997) Development of long-lifetime metal-ligand probes for biophysics and cellular imaging. J Fluoresc 7(1):17–25. doi:10.1007/bf02764573

49. Kellner K, Liebsch G, Klimant I, Wolfbeis OS, Blunk T, Schulz MB, Göpferich A (2002) Determination of oxygen gradients in engineered tissue using a fluorescent sensor. Biotechnol Bioeng 80(1):73–83. doi:10.1002/bit.10352

50. Gerencser AA, Neilson A, Choi SW, Edman U, Yadava N, Oh RJ, Ferrick DA, Nicholls DG, Brand MD (2009) Quantitative microplate-based respirometry with correction for oxygen diffusion. Anal Chem 81(16):6868–6878. doi:10.1021/ac900881z

51. McDonagh C, Burke CS, MacCraith BD (2008) Optical chemical sensors. Chem Rev 108(2):400–422. doi:10.1021/cr068102g

52. Wang X-d, Chen H-x, Zhao Y, Chen X, Wang X-r (2010) Optical oxygen sensors move towards colorimetric determination. Trends Anal Chem 29(4):319–338

53. Hogan MC (1999) Phosphorescence quenching method for measurement of intracellular in isolated skeletal muscle fibers. J Appl Physiol 86(2):720–724

54. Shonat RD, Kight AC (2003) Oxygen tension imaging in the mouse retina. Ann Biomed Eng 31(9):1084–1096. doi:10.1114/1.1603256

55. Fercher A, Ponomarev G, Yashunski D, Papkovsky D (2010) Evaluation of the derivates of phosphorescent Pt-coproporphyrin as intracellular oxygen-sensitive probes. Anal Bioanal Chem 396(5):1793–1803. doi:10.1007/s00216-009-3399-z

56. Zhang S, Hosaka M, Yoshihara T, Negishi K, Iida Y, Tobita S, Takeuchi T (2010) Phosphorescent light-emitting iridium complexes serve as a hypoxia-sensing probe for tumor imaging in living animals. Cancer Res 70(11):4490–4498. doi:10.1158/0008-5472.can-09-3948

57. Hynes J, Marroquin LD, Ogurtsov VI, Christiansen KN, Stevens GJ, Papkovsky DB, Will Y (2006) Investigation of drug-induced mitochondrial toxicity using fluorescence-based oxygen-sensitive probes. Toxicol Sci 92(1):186–200. doi:10.1093/toxsci/kfj208

58. Hynes J, Natoli E Jr, Will Y (2009) Fluorescent pH and oxygen probes of the assessment of mitochondrial toxicity in isolated mitochondria and whole cells. Curr Protoc Toxicol Chapter 2:Unit 2.16. doi:10.1002/0471140856.tx0216s40

59. Zitova A, O'Mahony FC, Cross M, Davenport J, Papkovsky DB (2009) Toxicological profiling of chemical and environmental samples using panels of test organisms and optical oxygen respirometry. Environ Toxicol 24(2):116–127. doi:10.1002/tox.20387

60. Dmitriev RI, Ropiak HM, Yashunsky DV, Ponomarev GV, Zhdanov AV, Papkovsky DB (2010) Bactenecin 7 peptide fragment as a tool for intracellular delivery of a phosphorescent oxygen sensor. FEBS J 277(22):4651–4661. doi:10.1111/j.1742-4658.2010.07872.x

61. Dmitriev RI, Zhdanov AV, Ponomarev GV, Yashunski DV, Papkovsky DB (2010) Intracellular oxygen-sensitive phosphorescent probes based on cell-penetrating peptides. Anal Biochem 398(1):24–33

62. Dmitriev RI, Ropiak H, Ponomarev G, Yashunsky DV, Papkovsky DB (2011) Cell-penetrating conjugates of coproporphyrins with oligoarginine peptides: rational design and application to sensing of intracellular O₂. Bioconj Chem. doi:10.1021/bc200324q

63. Foerg C, Merkle HP (2008) On the biomedical promise of cell penetrating peptides: limits versus prospects. J Pharm Sci 97(1):144–162. doi:10.1002/jps.21117

64. Koo Lee Y-E, Smith R, Kopelman R (2009) Nanoparticle PEBBLE sensors in live cells and in vivo. Annu Rev Anal Chem 2(1):57–76. doi:10.1146/annurev.anchem.1.031207.112823

65. Koo Lee Y-E, Ulbrich EE, Kim G, Hah H, Strollo C, Fan W, Gurjar R, Koo S, Kopelman R (2010) Near infrared luminescent oxygen nanosensors with nanoparticle matrix tailored sensitivity. Anal Chem 82(20):8446–8455. doi:10.1021/ac1015358

66. Coogan MP, Court JB, Gray VL, Hayes AJ, Lloyd SH, Millet CO, Pope SJA, Lloyd D (2010) Probing intracellular oxygen by quenched phosphorescence lifetimes of nanoparticles containing polyacrylamide-embedded [Ru(dpp(SO3Na)2)3]Cl2. Photochem Photobiolo Sci 9(1):103–109

67. Borisov SM, Mayr T, Mistlberger G, Waich K, Koren K, Chojnacki P, Klimant I (2009) Precipitation as a simple and versatile method for preparation of optical nanochemosensors. Talanta 79(5):1322–1330. doi:10.1016/j.talanta.2009.05.041

68. Chu C-S, Lo Y-L (2011) Highly sensitive and linear calibration optical fiber oxygen sensor based on Pt(II) complex embedded in sol-gel matrix. Sens Actuators B Chem 155(1):53–57

69. Wu C, Bull B, Christensen K, McNeill J (2009) Ratiometric single-nanoparticle oxygen sensors for biological imaging. Angew Chem Int Ed 48(15):2741–2745. doi:10.1002/anie.200805894

70. X-d Wang, Gorris HH, Stolwijk JA, Meier RJ, Groegel DBM, Wegener J, Wolfbeis OS (2011) Self-referenced RGB colour imaging of intracellular oxygen. Chem Sci 2(5):901–906

71. Fercher A, Borisov SM, Zhdanov AV, Klimant I, Papkovsky DB (2011) Intracellular O2 sensing probe based on cell-penetrating phosphorescent nanoparticles. ACS Nano 5:5499–5508. doi:10.1021/nn200807g

72. Napp J, Behnke T, Fischer L, Würth C, Wottawa M, Katschinski DM, Alves F, Resch-Genger U, Schäferling M (2011) Targeted luminescent near-infrared polymer-nanoprobes for in vivo imaging of tumor hypoxia. Anal Chem. doi:10.1021/ac201870b

73. Foster KA, Galeffi F, Gerich FJ, Turner DA, Müller M (2006) Optical and pharmacological tools to investigate the role of mitochondria during oxidative stress and neurodegeneration. Prog Neurobiol 79(3):136–171

74. Mik EG, Stap J, Sinaasappel M, Beek JF, Aten JA, van Leeuwen TG, Ince C (2006) Mitochondrial PO2 measured by delayed fluorescence of endogenous protoporphyrin IX. Nat Methods 3(11):939–945

75. Mik EG, Ince C, Eerbeek O, Heinen A, Stap J, Hooibrink B, Schumacher CA, Balestra GM, Johannes T, Beek JF, Nieuwenhuis AF, van Horssen P, Spaan JA, Zuurbier CJ (2009) Mitochondrial oxygen tension within the heart. J Mol Cell Cardiol 46(6):943–951

76. Harms FA, de Boon WM, Balestra GM, Bodmer SI, Johannes T, Stolker RJ, Mik EG (2011) Oxygen-dependent delayed fluorescence measured in skin after topical application of 5-aminolevulinic acid. J Biophotonics 4(10):731–739. doi:10.1002/jbio.201100040

77. Becker W, Su B, Holub O, Weisshart K (2010) FLIM and FCS detection in laser-scanning microscopes: increased efficiency by GaAsP hybrid detectors. Microsc Res Tech 74(9):804–811. doi:10.1002/jemt.20959

78. Takahashi E, Sato M (2010) Imaging of oxygen gradients in monolayer cultured cells using green fluorescent protein. Am J Physiol Cell Physiol 299(6):C1318–C1323. doi:10.1152/ajpcell.00254.2010

79. Schmalzlin E, van Dongen JT, Klimant I, Marmodee B, Steup M, Fisahn J, Geigenberger P, Lohmannsroben HG (2005) An optical multifrequency phase-modulation method using microbeads for measuring intracellular oxygen concentrations in plants. Biophys J 89(2):1339–1345. doi:10.1529/biophysj.105.063453

80. O'Riordan TC, Zhdanov AV, Ponomarev GV, Papkovsky DB (2007) Analysis of intracellular oxygen and metabolic responses of mammalian cells by time-resolved fluorometry. Anal Chem 79(24):9414–9419. doi:10.1021/ac701770b

81. Fercher A, O'Riordan TC, Zhdanov AV, Dmitriev RI, Papkovsky DB (2010) Imaging of cellular oxygen and analysis of metabolic responses of mammalian cells. Methods Mol Biol 591:257–273. doi:10.1007/978-1-60761-404-3_16

82. Sharman KK, Periasamy A, Ashworth H, Demas JN, Snow NH (1999) Error analysis of the rapid lifetime determination method for double-exponential decays and new windowing schemes. Anal Chem 71(5):947–952

83. Zhdanov A, Dmitriev R, Papkovsky D (2011) Bafilomycin A1 activates respiration of neuronal cells via uncoupling associated with flickering depolarization of mitochondria. Cell Mol Life Sci 68(5):903–917. doi:10.1007/s00018-010-0502-8

84. Zhdanov AV, Ogurtsov VI, Taylor CT, Papkovsky DB (2010) Monitoring of cell oxygenation and responses to metabolic stimulation by intracellular oxygen sensing technique. Integr Biol 2(9):443–451

85. Zhdanov AV, Ward MW, Prehn JHM, Papkovsky DB (2008) Dynamics of intracellular oxygen in PC12 cells upon stimulation of neurotransmission. J Biol Chem 283(9):5650–5661. doi:10.1074/jbc.M706439200

86. Zhdanov AV, Ward MW, Taylor CT, Souslova EA, Chudakov DM, Prehn JH, Papkovsky DB (2010) Extracellular calcium depletion transiently elevates oxygen consumption in neurosecretory PC12 cells through activation of mitochondrial Na^+/Ca^{2+} exchange. Biochim Biophys Acta 1797(9):1627–1637. doi:10.1016/j.bbabio.2010.06.006

87. Ceroni P, Lebedev AY, Marchi E, Yuan M, Esipova TV, Bergamini G, Wilson DF, Busch TM, Vinogradov SA (2011) Evaluation of phototoxicity of dendritic porphyrin-based phosphorescent oxygen probes: an in vitro study. Photochem Photobiol Sci 10(6):1056–1065. doi:10.1039/c0pp00356e

88. Papkovsky DB (ed) (2010) Live cell imaging methods and protocols, vol 591. Methods in Molecular Biology. Humana Press, New York

89. Won Y, Moon S, Yang W, Kim D, Han WT, Kim DY (2011) High-speed confocal fluorescence lifetime imaging microscopy (FLIM) with the analog mean delay (AMD) method. Opt Express 19(4):3396–3405

90. Schneckenburger H, Wagner M, Weber P, Bruns T, Richter V, Strauss WS, Wittig R (2010) Multi-dimensional fluorescence microscopy of living cells. J Biophotonics. doi:10.1002/jbio.201000098

91. Lebedev AY, Cheprakov AV, SakadzÌŒicÌ S, Boas DA, Wilson DF, Vinogradov SA (2009) Dendritic phosphorescent probes for oxygen imaging in biological systems. ACS Appl Mater Interfaces 1(6):1292–1304. doi:10.1021/am9001698

92. Sakadzic S, Roussakis E, Yaseen MA, Mandeville ET, Srinivasan VJ, Arai K, Ruvinskaya S, Devor A, Lo EH, Vinogradov SA, Boas DA (2010) Two-photon high-resolution measurement of partial pressure of oxygen in cerebral vasculature and tissue. Nat Methods 7(9):755–759

93. Greger K, Neetz MJ, Reynaud EG, Stelzer EH (2011) Three-dimensional fluorescence lifetime imaging with a single plane illumination microscope provides an improved signal to noise ratio. Opt Express 19(21):20743–20750 pii: 222944

94. Finikova OS, Lebedev AY, Aprelev A, Troxler T, Gao F, Garnacho C, Muro S, Hochstrasser RM, Vinogradov SA (2008) Oxygen microscopy by two-photon-excited phosphorescence. ChemPhysChem 9(12):1673–1679. doi:10.1002/cphc.200800296

95. Ashkenazi S, Huang S-W, Horvath T, Koo Y-EL, Kopelman R (2008) Photoacoustic probing of fluorophore excited state lifetime with application to oxygen sensing. J Biomedical Optics 13(3):034023–034024

96. Koo Y-EL, Cao Y, Kopelman R, Koo SM, Brasuel M, Philbert MA (2004) Real-time measurements of dissolved oxygen inside live cells by organically modified silicate fluorescent nanosensors. Anal Chem 76(9):2498–2505. doi:10.1021/ac035493f

97. Gupta B, Levchenko TS, Torchilin VP (2005) Intracellular delivery of large molecules and small particles by cell-penetrating proteins and peptides. Adv Drug Deliv Rev 57(4):637–651. doi:10.1016/j.addr.2004.10.007

98. Torchilin VP (2006) Recent approaches to intracellular delivery of drugs and DNA and organelle targeting. Annu Rev Biomed Eng 8:343–375. doi:10.1146/annurev.bioeng.8.061505.095735

99. Nishiyama N, Nakagishi Y, Morimoto Y, Lai PS, Miyazaki K, Urano K, Horie S, Kumagai M, Fukushima S, Cheng Y, Jang WD, Kikuchi M, Kataoka K (2009) Enhanced photodynamic cancer treatment by supramolecular nanocarriers charged with dendrimer phthalocyanine. J Control Release 133(3):245–251. doi:10.1016/j.jconrel.2008.10.010

100. Rancan F, Wiehe A, Nobel M, Senge MO, Omari SA, Bohm F, John M, Roder B (2005) Influence of substitutions on asymmetric dihydroxychlorins with regard to intracellular uptake, subcellular localization and photosensitization of Jurkat cells.

J Photochem Photobiol B 78(1):17–28. doi:10.1016/j.jphotobiol.2004.08.010

101. Golub AS, Barker MC, Pittman RN (2007) PO2 profiles near arterioles and tissue oxygen consumption in rat mesentery. Am J Physiol Heart Circu Physiol 293(2):H1097–H1106. doi:10.1152/ajpheart.00077.2007

102. Golub AS, Pittman RN (2008) PO2 measurements in the microcirculation using phosphorescence quenching microscopy at high magnification. Am J Physiol Heart Circu Physiol 294(6):H2905–H2916. doi:10.1152/ajpheart.01347.2007

103. Golub AS, Tevald MA, Pittman RN (2011) Phosphorescence quenching microrespirometry of skeletal muscle in situ. Am J Physiol Heart Circu Physiol 300(1):H135–H143. doi:10.1152/ajpheart.00626.2010

104. Pittman RN, Golub AS, Carvalho H (2010) Measurement of oxygen in the microcirculation using phosphorescence quenching microscopy Oxygen Transport to Tissue XXXI. In: Takahashi E, Bruley DF (eds), vol 662. Advances in Experimental Medicine and Biology. Springer US, pp 157-162. doi:10.1007/978-1-4419-1241-1_22

105. Vanderkooi JM, Maniara G, Green TJ, Wilson DF (1987) An optical method for measurement of dioxygen concentration based upon quenching of phosphorescence. J Biol Chem 262(12):5476–5482

106. Lo L-W, Koch CJ, Wilson DF (1996) Calibration of oxygen-dependent quenching of the phosphorescence of Pd-meso-tetra (4-carboxyphenyl) porphine: a phosphor with general application for measuring oxygen concentration in biological systems. Anal Biochem 236(1):153–160. doi:10.1006/abio.1996.0144

107. Estrada AD, Ponticorvo A, Ford TN, Dunn AK (2008) Microvascular oxygen quantification using two-photon microscopy. Opt Lett 33(10):1038–1040

108. Wilson DF, Vinogradov SA, Grosul P, Sund N, Vacarezza MN, Bennett J (2006) Imaging oxygen pressure in the rodent retina by phosphorescence lifetime. In: Oxygen transport to tissue XXVII, vol 578. Advances in experimental medicine and biology. Springer, US, pp 119–124. doi:10.1007/0-387-29540-2_19

109. Zhdanov AV, Favre C, O'Flaherty L, Adam J, O'Connor R, Pollard PJ, Papkovsky DB (2011) Comparative bioenergetic assessment of transformed cells using a cell energy budget platform. Integr Biol 3(11):1135–1142

110. Lebedev AY, Troxler T, Vinogradov SA (2008) Design of metalloporphyrin-based dendritic nanoprobes for two-photon microscopy of oxygen. J Porphyr Phthalocyanines 12(12):1261–1269. doi:10.1142/S1088424608000649

111. Esipova TV, Karagodov A, Miller J, Wilson DF, Busch TM, Vinogradov SA (2011) Two new "Protected" oxyphors for biological oximetry: properties and application in tumor imaging. Anal Chem. doi:10.1021/ac2022234

112. Wotzlaw C, Bernardini A, Berchner-Pfannschmidt U, Papkovsky D, Acker H, Fandrey J (2011) Multifocal animated imaging of changes in cellular oxygen and calcium concentrations and membrane potential within the intact adult mouse carotid body ex vivo. Am J Physiol Cell Physiol. doi:10.1152/ajpcell.00508.2010

113. Huppert TJ, Allen MS, Benav H, Jones PB, Boas DA (2007) A multicompartment vascular model for inferring baseline and functional changes in cerebral oxygen metabolism and arterial dilation. J Cereb Blood Flow Metab 27(6):1262–1279

114. Fang Q, Sakadzic S, Ruvinskaya L, Devor A, Dale AM, Boas DA (2008) Oxygen advection and diffusion in a three-dimensional vascular anatomical network. Opt Express 16(22):17530–17541

115. Zheng L, Golub AS, Pittman RN (1996) Determination of PO₂ and its heterogeneity in single capillaries. Am J Physiol Heart Circ Physiol 271(1):H365–H372

116. Yaseen MA, Srinivasan VJ, Sakadzic S, Wu W, Ruvinskaya S, Vinogradov SA, Boas DA (2009) Optical monitoring of oxygen tension in cortical microvessels with confocal microscopy. Opt Express 17(25):22341–22350. doi:10.1364/OE.17.022341

117. Sinks LE, Roussakis E, Esipova TV, Vinogradov SA (2010) Synthesis and calibration of phosphorescent nanoprobes for oxygen imaging in biological systems. J Vis Exp (37):e1731

118. Howlett RA, Kindig CA, Hogan MC (2007) Intracellular PO₂ kinetics at different contraction frequencies in Xenopus single skeletal muscle fibers. J Appl Physiol 102(4):1456–1461. doi:10.1152/japplphysiol.00422.2006

119. Gupta K, Kim D-H, Ellison D, Smith C, Kundu A, Tuan J, Suh K-Y, Levchenko A (2011) Lab-on-a-chip devices as an emerging platform for stem cell biology. Lab Chip 10(16):2019–2031

120. Will Y, Hynes J, Ogurtsov VI, Papkovsky DB (2006) Analysis of mitochondrial function using phosphorescent oxygen-sensitive probes. Nat Protoc 1(6):2563–2572. doi:10.1038/nprot.2006.351

121. Huang B, Babcock H, Zhuang X (2010) Breaking the diffraction barrier: super-resolution imaging of cells. Cell 143(7):1047–1058